# Preprints

# 2nd IFAC Workshop on Fractional Differentiation and its Applications

## 19 - 21 July, 2006
## Porto, Portugal

IFAC    isep    INSTITUTO POLITÉCNICO DO PORTO    FCT

Instituto superior de engenharia do porto

Proceedings of the 2nd IFAC
Workshop on Fractional Differentiation and its Applications
Porto, Portugal, July 19-21, 2006

# FRACTIONAL DYNAMICS IN GENETIC ALGORITHMS

**E. J. Solteiro Pires** [*] **J. A. Tenreiro Machado** [**]
**P. B. de Moura Oliveira** [*]

[*] *Dep. de Eng. Electrotécnica, Universidade de Trás-os-Montes
e Alto Douro,Quinta de Prados, 5000–911 Vila Real, Portugal*
[**] *Dep. Eng. Electrotécnica, Inst. Superior de Engenharia do
Porto, R. Dr Ant. Bernadino Almeida, 4200–072 Porto, Portugal*

Abstract: This paper investigate the fractional-order dynamics during the evolution of a Genetic Algorithm (GA). In order to study the phenomena involved in the GA population evolution, the mutation is exposed to excitation perturbations during some generations and the corresponding fitness variations are evaluated. Three similar functions are tested to measure its influence in GA dynamics. The input and output signals are studied revealing a fractional-order dynamic evolution.

Keywords: Genetic Algorithms, Fractional Order, Dynamics

## 1. INTRODUCTION

In the last twenty years Genetic Algorithms (GAs) have been applied in a plethora of fields such as in image processing, pattern recognition, speech recognition, control, system identification, optimization, planning and scheduling (Bäck *et al.*, 1997). While GAs have proved to be a valuable optimization tool in solving a wide range of problems, its dynamic are not yet fully studied, particulary in terms of the influence of perturbation signals.

Fractional Calculus (FC) is a natural extension of the classical mathematics. In fact, since the beginning of theory of differential and integral calculus, several mathematicians investigated the calculation of non-integer order derivatives and integrals. Nevertheless, the application of FC has been scarce until recently, but the advances in the theory of chaos motivated a renewed interest in this field.

Bearing these ideas in mind, this paper analyzes the system signal evolution and the fractional-order dynamics in the population of a GA-based optimization. The article is organized as follows. Section 2 introduces the problem and the GA method for its reso-
lution. Based on this formulation, section 3 presents the results for several simulations involving different working conditions and studies the resultant dynamic phenomena. Section 4 presents the results for other functions. Finally, section 5 outlines the main conclusions.

## 2. THE OPTIMIZATION GA

This section presents the *optimization* GA used in the study of the dynamic system. The objective function consists on minimizing the function (1). This function has only one parameter and a binary Gray code, with the string length of $l = 24$ bits, is used to represent the solutions of the population (2). The parameter $b$ can vary in the interval $[-50000, 50000]$.

$$f_A(b) = 1 + |b - 41| \qquad (1)$$

$$b = \{b_1, b_2, b_3, \ldots, b_l\} \qquad (2)$$

A 50–population GA is run during 200 generations under rank selection with simple crossover and mu-

tation with probabilities $p_c = 0.8$ and $p_m = 0.05$, respectively. The best solution of each generations is always passed to the next generation.

The influence of several factors can be analyzed in order to study the dynamics of the GA, particulary the probabilities. This influence can be distinct to the type of selection, elitism, fitness function and string length used in the GA. In this work, across each test function experiment, it is changed only the initial seed of the mutation probability noise that is added to $p_m$.

## 3. EVOLUTION, SIGNAL PROPAGATION AND FRACTIONAL-ORDER DYNAMICS

This section studies the dynamical phenomena involved in the signal propagation in the GA population. In this perspective, small amplitude perturbations are superimposed over biasing signals of the GA system and its influence on the population fitness is evaluated. The experiments reveal a fractional-order dynamics capable of being described by systems theory tools.

### 3.1 The GA dynamics

In this section the GA system is stimulated by perturbing the mutation probability, $p_m$, through a white noise signal, $\delta p_m$, and the corresponding population fitness modification $\delta f$ is evaluated, see figure 1. The crossover and other probability signals used, $p_c$ and $p_o$, remain unchanged. Therefore, the variation of the mutation probability and the resulting fitness modification on the GA population, during the evolution, can be viewed as the system inputs and output signals varying during the successive generations. This analysis is evaluated using several experiments with different seeds for a small amplitude white noise perturbation signal. All the other seeds remain unchanged.
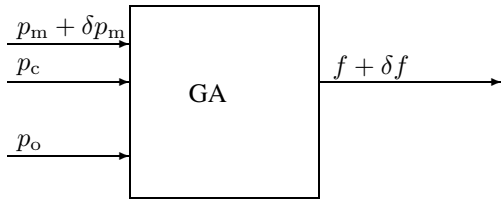


Fig. 1. System dynamics

In this perspective, a white noise signal $\delta p_m(T)$ is added to the mutation probability $p_m$ of the strings during a time period $T_{exc}$ and the new mutation probability $p_{m\,noise}$ is calculated by:

$$p_{m\,noise} = \begin{cases} 0 & \text{if } p_m + \eta(\Delta p) < 0 \\ 1 & \text{if } p_m + \eta(\Delta p) > 1 \quad (3) \\ p_m + \eta(\Delta p) & \text{otherwise} \end{cases}$$

where $\eta$ is the white noise signal with maximum amplitude $\pm \Delta p$.

Consequently, the input signal, at generation $T$, is the difference between the two cases, that is $\delta p_m(T) = p_{m\,noise}(T) - p_m(T)$. On the other hand, the output signal is the difference in the population fitness with and without noise, that is $\delta f(T) = f_{m\,noise}(T) - f(T)$.

Figure 2 shows the input signal $\delta p_m(T)$, with seed $i = 1$, in the generation domain and the corresponding polar diagram, for $\Delta p = 0.04$ and $T_{exc} = 2$, where $\mathscr{F}[\delta p_m(T)]$ represents the Fourier transform of the signal perturbation. Figure 3 show the corresponding output signal variation $\delta f(T)$.
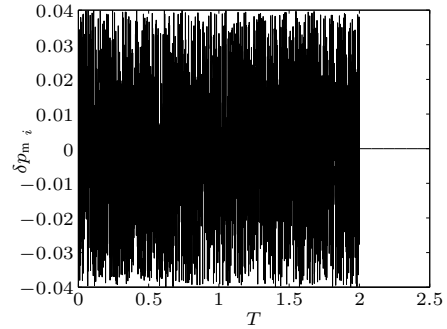


(a) Generation domain
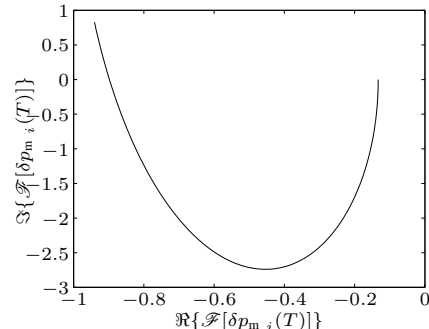


(b) Polar diagram

Fig. 2. Input signal $\delta p_m$ perturbation over $T_{exc} = 2$ generations with seed $i = 1$ ($\Delta p = 0.04$)

Once having de Fourier description of the input and output signals it is possible to calculate the corresponding transfer function (4) for seed $i$.

$$H_i(jw) = \frac{\mathscr{F}\{\delta f_i(T)\}}{\mathscr{F}\{\delta p_{m\,i}(T)\}} \qquad (4)$$

The transfer function $H_1(jw)$, with seed $i = 1$, between the input and output signals, is depicted in figure 4.

After repeating for all seeds a 'representative' transfer function is obtained by using the median of the statistical sample (Tenreiro Machado and Galhano, 1998) of $n$ experiments (see figure 5).
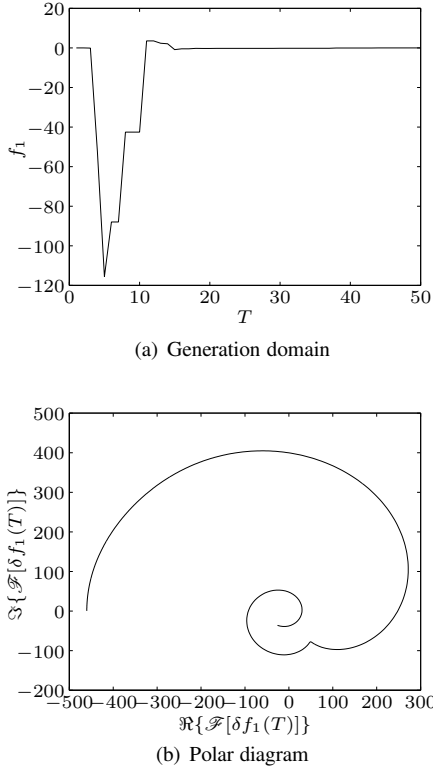
440
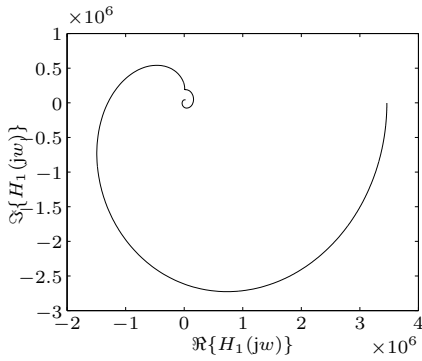
## 3.2 Transfer function identification

In this section the median of the numerical system transfer functions, figure 6, is approximated by analytical expressions with gain $\kappa \in \mathbb{R}^+$ and two poles $(a, b) \in \mathbb{R}^+$ of fractional orders $(\alpha, \beta) \in \mathbb{R}^+$, respectively, given by equation (5):

$$G_A(\mathrm{j}w) = \frac{\kappa}{\left(\frac{\mathrm{j}w}{a} + 1\right)^\alpha \left[\left(-\frac{\mathrm{i}w}{b}\right)^\beta + 1\right]} \qquad (5)$$

It is worth notice that the transfer function has a pole in the right half plane. It is known that in fractional systems, for a given root $z$ of multiplicity $\beta$, the stability criterion is $\arg(z) > \beta\pi/2$. In the present case, depending on the numerical values of the parameters, it can occur that the identified transfer function corresponds to an unstable system; however, such behavior was not observed. Moreover, many other expressions were attempted for the transfer function leading, in all cases, to a clearly inferior identification. Therefore, it remains to be further investigated either the physical reason justifying this expression or, alternatively, the construction of another expression leading to similar good estimation while avoiding this intricate problem.

In order to estimate the transfer function parameters, an *identification* GA adopting a real string is executed with the representation $\{k, a, b, \alpha, \beta\}$. The *identification* GA is executed during $T_{ide} = 600$ generations with a 100 strings population. It is used the simulated binary crossover (Deb, 2001) and, when one mutation occurs, the corresponding value $\{x_1,...,x_5\} \equiv \{k, a, b, \alpha, \beta\}$ is changed according with the equations:

$$x_{i+1} = 10^{u_i} x_i \qquad (6a)$$

$$u_i \sim \mathrm{U}[-\varepsilon_i, +\varepsilon_i] \qquad (6b)$$

where $u_i$ is a random number generated through the uniform probability distribution U and $\varepsilon_i$ is fixed according with the range of estimation.

The fitness function $f_{ide}$ measures the distance between the median $H(\mathrm{j}w_k)$ and $G(\mathrm{j}w_k)$:

$$f_{ide} = \sum_{k=1}^{nf} \| H(\mathrm{j}w_k) - G(\mathrm{j}w_k) \| \qquad (7)$$

where $H$ represents the median of the $n$ transfer functions resulting for each different seed, $nf$ is the total number of sampling points and $w_k$, $k = \{1, ..., nf\}$ is the corresponding vector of frequencies.

Since the *optimization* GA has a stochastic dynamics, every time the GA is executed with a different white noise seed, leads to a different transfer function. Consequently, in order to obtain a numerical convergence (Tenreiro Machado and Galhano, 1998) are performed



(a) Generation domain



(b) Polar diagram

Fig. 3. Output variation $\delta f(T)$ for the input excitation over $T_{exc} = 2$ generations with seed $i = 1$ ($\Delta p = 0.04$)



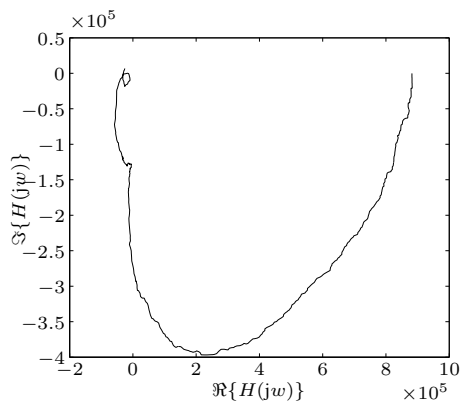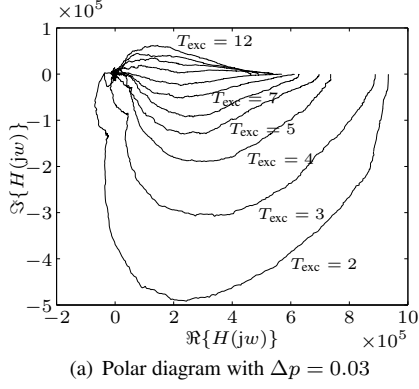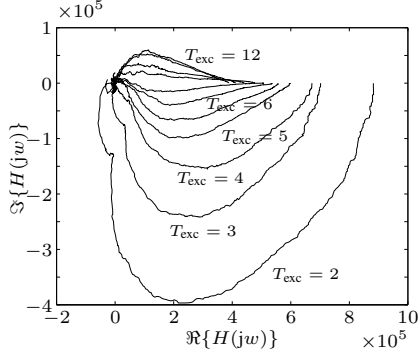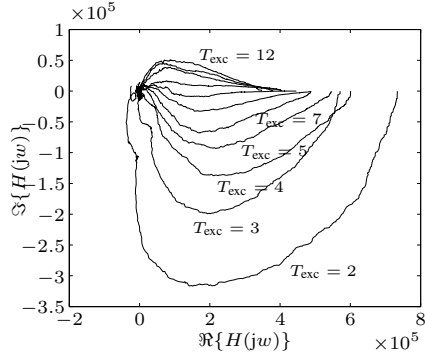Fig. 4. Transfer function $H_1(\mathrm{j}w)$ using seed $i = 1$ ($T_{exc} = 2$, $\Delta p = 0.04$)



Fig. 5. Median transfer function $H(\mathrm{j}w)$ ($T_{exc} = 2$, $\Delta p = 0.04$)

(a) Polar diagram with $\Delta p = 0.03$


(b) Polar diagram with $\Delta p = 0.04$


(c) Polar diagram with $\Delta p = 0.05$

Fig. 6. Polar diagrams of $H(jw)$ for $\Delta p = \{0.03, 0.04, 0.05\}$

$n = 1701$ perturbation experiments with different seeds for the white noise signal, $\delta p_{\mathrm{m}}(T)$ (all the other seeds for $p_{\mathrm{m}}$, $p_{\mathrm{c}}$ and selection remains unchanged). So, the transfer function of the optimization GA dynamics is evaluated by computing the Fourier transform (FT) for each pair of input and output signals. After that, the medians of the transfer functions calculated previously (*i.e.*, for each real and imaginary part and for each frequency) are taken as the final part of the numerical transfer function $H(jw)$ (see figure 6).

For evaluating the influence of the excitation period $T_{\mathrm{exc}}$ several simulations are performed ranging from $T_{\mathrm{exc}} = 2$ up to $T_{\mathrm{exc}} = 12$ generations. Therefore, the relation between the transfer function parameters and $T_{\mathrm{exc}}$ are shown in figures 7–8.

The charts of $\{\kappa, a, b, \alpha, \beta\}$ can be approximated using equation (8) leading to the parameters of table 1.
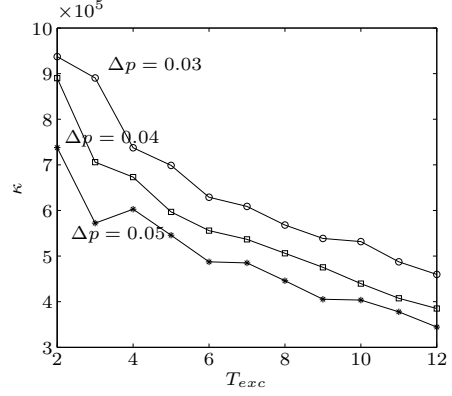

Fig. 7. Estimated gain $\kappa$ *vs.* $T_{exc}$

Table 1. Parameters of $\gamma_i$, $i = \{1, 2\}$ approximation of $f_A$ optimization fuction

| $\Delta p$ | | 0.03 | 0.04 | 0.05 |
|---|---|---|---|---|
| $\kappa$ | $\gamma_1 (10^5)$ | 10.0 | 10.0 | 9.7 |
| | $\gamma_2$ | $-0.40$ | $-0.44$ | $-0.39$ |
| $a$ | $\gamma_1$ | 2.90 | 2.12 | 2.50 |
| | $\gamma_2$ | $-1.40$ | $-1.26$ | $-1.31$ |
| $\alpha$ | $\gamma_1$ | 10.86 | 7.42 | 7.23 |
| | $\gamma_2$ | $-1.26$ | $-1.11$ | $-1.10$ |
| $b$ | $\gamma_1$ | 0.93 | 1.14 | 1.16 |
| | $\gamma_2$ | $-0.67$ | $-0.76$ | $-0.79$ |
| $\beta$ | $\gamma_1$ | 0.83 | 0.75 | 0.75 |
| | $\gamma_2$ | 0.04 | 0.09 | 0.10 |

$$\{\kappa, a, \alpha, b, \beta\} \simeq \gamma_1 \, (T_{exc})^{\gamma_2} \qquad (8)$$

These results reveal that the transfer function parameters $\{\kappa, a, \alpha, b, \beta\}$ vary with a power law *versus* the excitation time $T_{\mathrm{exc}}$. The right half-plane pole $b$ has a low dependence with $T_{\mathrm{exc}}$ and, consequently, the adoption of a particular value for $T_{\mathrm{exc}}$ is of no importance for the study under effect. On the other hand, the left half-plane pole $a$ has a much stronger influence on the transfer function. Furthermore, $\kappa$ varies with $\Delta p$ while $a, \alpha, b, \beta$ have a low dependence with $\Delta p$.

By enabling the zero/pole order to vary freely, we get non-integer values for $\alpha$ and $\beta$, while the adoption of an integer-order transfer function would lead to a larger number of zero/poles to get the same quality in the analytical fitting to the numerical values. The 'requirement' of fractional-order models in opposition with the classical case of integer models is a well-known discussion and even nowadays final conclusions are not clear since it is always possible to approximate a fractional frequency response through an integer one as long as we make use of a larger number of zeros and poles. Nevertheless, in the present experiments there is a complementary point of view towards FC.
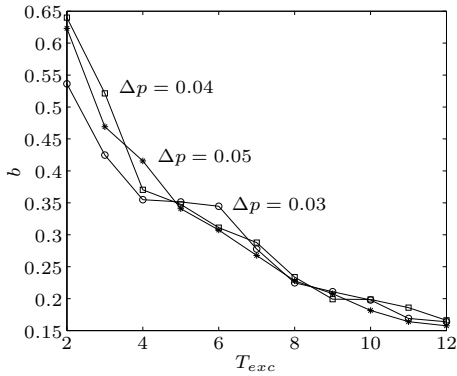
## 4. ADDITIONAL EXPERIMENTS

This section presents the results when using different fitness functions (9) in the optimization GA, in order to investigate its relation with the transfer function.
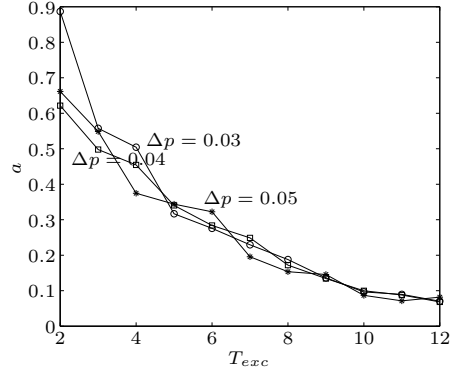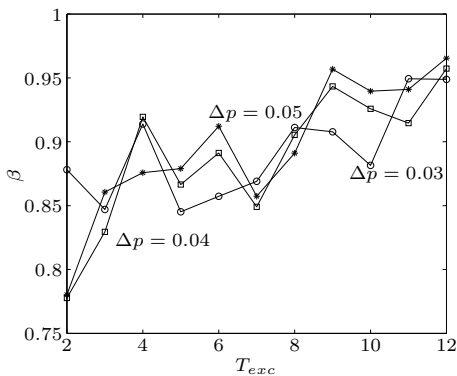
(a) Estimated pole $a$ *vs.* $T_{exc}$
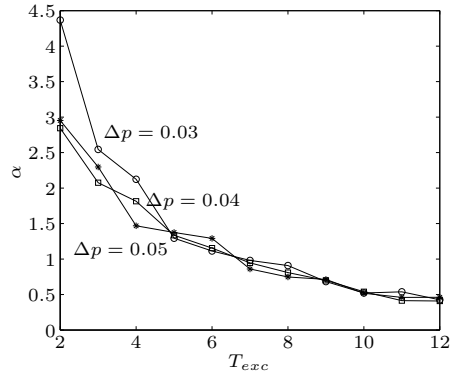


(b) Estimated pole fractional-order $\alpha$ *vs.* $T_{\text{exc}}$



(c) Estimated pole $b$ *vs.* $T_{\text{exc}}$



(d) Estimated pole fractional-order $\beta$ *vs.* $T_{\text{exc}}$

Fig. 8. Estimated poles and fractional-orders *vs.* $T_{\text{exc}}$

Table 2. Parameters of $\gamma_i$, $i = \{1, 2\}$ approximation of $f_B$ optimization function

| $\Delta p$ | | 0.03 | 0.04 | 0.05 |
|---|---|---|---|---|
| $\kappa$ | $\gamma_1(10^8)$ | 6 | 5 | 4 |
| | $\gamma_2$ | $-0.40$ | $-0.38$ | $-0.30$ |
| $a$ | $\gamma_1$ | 6.39 | 4.66 | 6.83 |
| | $\gamma_2$ | $-2.26$ | $-2.03$ | $-2.27$ |
| $\alpha$ | $\gamma_1$ | 6.87 | 5.65 | 7.39 |
| | $\gamma_2$ | $-1.44$ | $-1.25$ | $-1.40$ |
| $b$ | $\gamma_1$ | 2.02 | 1.93 | 1.42 |
| | $\gamma_2$ | $-1.05$ | $-1.09$ | $-0.95$ |
| $\beta$ | $\gamma_1$ | 0.70 | 0.66 | 0.70 |
| | $\gamma_2$ | 0.11 | 0.15 | 0.12 |

Table 3. Parameters of $\gamma_i$, $i = \{1, 2\}$ approximation of $f_C$ optimization function

| $\Delta p$ | | 0.03 | 0.04 | 0.05 |
|---|---|---|---|---|
| $\kappa$ | $\gamma_1(10^{11})$ | 4 | 3 | 3 |
| | $\gamma_2$ | $-0.50$ | $-0.39$ | $-0.27$ |
| $a$ | $\gamma_1$ | 6.83 | 6.00 | 4.14 |
| | $\gamma_2$ | $-2.35$ | $-2.33$ | $-2.12$ |
| $\alpha$ | $\gamma_1$ | 6.91 | 5.78 | 3.89 |
| | $\gamma_2$ | $-1.46$ | $-1.35$ | $-1.08$ |
| $b$ | $\gamma_1$ | 1.49 | 1.60 | 1.51 |
| | $\gamma_2$ | $-0.98$ | $-1.06$ | $-1.09$ |
| $\beta$ | $\gamma_1$ | 0.74 | 0.70 | 0.70 |
| | $\gamma_2$ | 0.09 | 0.10 | 0.11 |

The study follows an identical strategy to the one adopted in the work of previous section.

$$f_B(b) = 1 + |b - 41|^2 \qquad (9a)$$

$$f_C(b) = 1 + |b - 41|^3 \qquad (9b)$$

The polar diagrams obtained and its estimated parameters $\{\kappa, a, \alpha, b, \beta\}$ for $f_B$ and $f_C$ are similar with the previous obtained to $f_A$. These parameters can be approximated also through the power expressions (8) leading to the results shown in tables 2-3.

To study the influence of the fitness function in the *optimization* GA, the median of each parameter is evaluated for all optimization functions and taken as the representative parameter of that function. These estimated parameters are compared in figures 9-10. As can be seen the parameters have a similar behavior. The $\kappa$ gain varies with the power used in the *optimization* function. On the other hand, the concavity of the $\{a, \alpha\}$ parameters increases as the power used in the function increases.

## 5. CONCLUSIONS

This paper analyzed the signal propagation and the dynamic phenomena involved in the time evolution of a population of individuals. The study was established on the basis of a simple GA function optimization. While the study of GA schemes has been extensively studied, the influence of perturbation signals over the operating conditions is not well known.
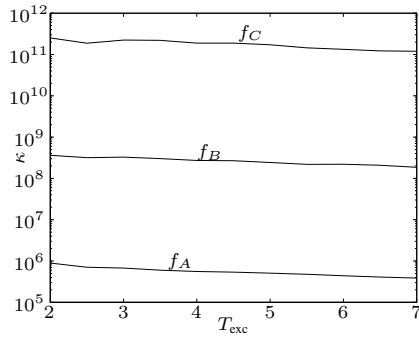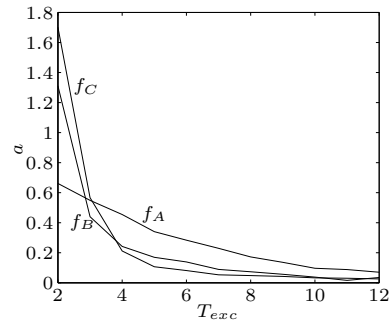
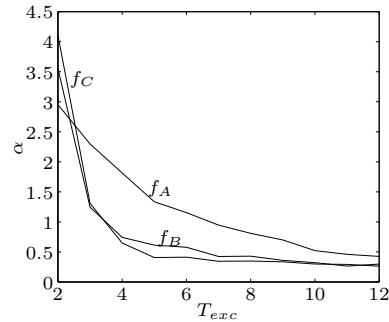Fig. 9. Median of the estimated parameter $\kappa$ vs. $T_{\text{exc}}$ for $\{f_A, f_B, f_C\}$

Bearing these ideas in mind, the fractional calculus perspective calculus was introduced in order to develop simple, but comprehensive, approximating transfer functions of non-integer order. It was shown that fractional models capture phenomena and properties that classical integer-order overlook.

.

## REFERENCES

Bäck, Thomas, Ulrich Hammel and Hans-Paul Schwefel (1997). Evolutionary computation: Comments on the history and current state. *IEEE Trans. on Evolutionary Computation* **1**(1), 3–17.

Deb, Kalyanmoy (2001). *Multi-Objective Optimization Using Evolutionary Algorithms*. John Wiley & Sons, LTD.

Gement, Andrew (1938). On fractional differentials. *Proc. Philosophical Magazine* **25**, 540–549.

Méhauté, Alain Le (1991). *Fractal Geometries: Theory and Applications*. Penton Press.

Oustaloup, A. (1991). *La Commande CRONE: Commande Robuste d'Ordre Non Intier*. Hermes.

Podlubny, I. (1999). *Fractional Diferential Equations*. Academic Press. San Diego.

Solteiro Pires, E. J., J. A. T Machado and P. B. M. Oliveira (2003). Fractional order dynamics in a GA planner. *Signal Process.* **83**(11), 2377–2386.

Solteiro Pires, E. J., J. A. Tenreiro Machado and P. B. de Moura Oliveira (2006). Dynamical modelling of a genetic algorithm. *Signal Process.*

Tenreiro Machado, J. (1997). Analysis and design of fractional-order digital control systems. *J. Syst. Analysis-Modelling-Simulation* **27**, 107–122.

Tenreiro Machado, J. A. (2001). Syst. modeling and control through fractional-order algorithms. *FCAA – Journal of Fractional Calculus & Ap. Analysis* **4**, 47–66.

Tenreiro Machado, J. and A.M.S. F. Galhano (1998). A statistical perspective to the fourier analysis of mechanical manipulators. *Journal Systems Analysis-Modelling-Simulation* **33**, 373–384.

Torvik, P. J. and R. L. Bagley (1984). On the appearance of the fractional derivative in the behaviour of real materials. *ASME Journal of Applied Mechanics* **51**, 294–298.
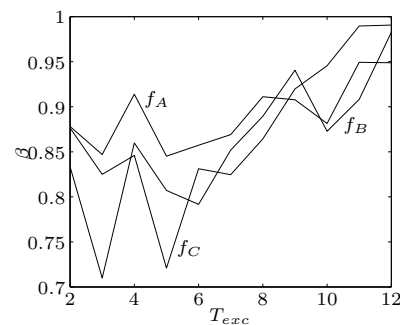
(a) Median of the estimated parameter $a$ vs. $T_{\text{exc}}$



(b) Median of the estimated parameter $\alpha$ vs. $T_{\text{exc}}$
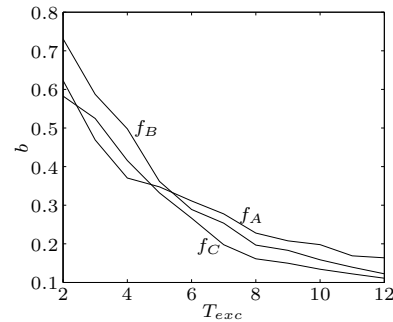


(c) Median of the estimated parameter $b$ vs. $T_{\text{exc}}$



(d) Median of the estimated parameter $\beta$ vs. $T_{\text{exc}}$

Fig. 10. Median of estimated poles and fractional-orders vs. $T_{\text{exc}}$ for $\{f_A, f_B, f_C\}$

Vinagre, B. M., I. Petras, I. Podlubny and Y. Q. Chen (2002). Using fractional order adjustment rules and fractional order reference models in model-reference adaptive control. *Nonlinear Dynamics* **1-4**(29), 269–279.

Westerlund, Svante (2002). *Dead Matter Has Memory! Causal Consulting*. Kalmar. Sweden.